Comparison of Micro Arc Oxidation and Friction Stir Processed Coatings on Aluminum Alloys

*Sudhir Baral, Raghu Raj Rangaraju, Mr. Anand Patil, Prasad Rao Kalvala, K.S. Raja & M. Misra**
Chemical & Metallurgical Engineering
University of Nevada-Reno
Reno, Nevada USA

Surface composite coatings were developed on aluminum alloys (Al-2% Mg) using micro-arc oxidation (MAO) and friction stir processing (FSP) techniques. MAO coatings were developed by applying 400-V, direct current between the substrate and a titanium cathode. A silicate predominant alkaline solution was used as the electrolyte. FSP coatings were developed by embedding SiC particles into the matrix. A steel tool with a pin was used for processing. The corrosion resistance was assessed by electrochemical impedance spectroscopy (EIS) and salt spray testing. The wear resistance was determined by the pin-on-disk method. The results showed that both MAO and FSP coatings exhibited an increase in wear resistance compared to the uncoated base metal. By contrast, the corrosion resistance of MAO coatings was found to be significantly higher than the FSP coatings and uncoated basis metal. Impedance values at the lower frequency for the FSP coatings and the basis metal were in the range of 100 to 180 Ω, whereas for the MAO-coated samples, it was 12×10^7 Ω. Based on this study, MAO coatings are recommended for obtaining both wear and corrosion resistance on aluminum alloys. The results were substantiated by SEM analysis.

Keywords: *Micro-arc oxidation coatings, friction-stir processed coatings, composite coatings, coating of aluminum alloys, wear resistance, corrosion resistance.*

Introduction

Aluminum alloys are extremely useful for many industrial applications, especially in automotive and aerospace applications, because they are relatively inexpensive, lighter and exhibit an excellent strength-to-weight ratio. However, the major drawback of aluminum alloys is that they are chemically active whereby they react with chemicals and even moisture in the air, and corrode. Further, they wear easily because of their relative softness. Therefore, surface treatments are necessary to protect them against corrosion and wear.

Recently, considerable interest has developed in a micro-arc oxidation (MAO) (also referred to as plasma electrolytic oxidation (PEO) and spark discharge anodizing) technique as a promising surface treatment for aluminum and magnesium alloys for hexavalent chromium replacement in corrosion protection[1-4] as well as improving the tribological properties of the alloys.[5-9] Essentially, it involves the modification of a conventional anodically grown oxide film by the application of an electric field stronger than the dielectric breakdown field for the oxide. Discharges occur, and the resulting plasma-chemical reactions contribute to the growth of the coating. More significantly, local conditions of heat and pressure sinter and anneal the coating. Rapid cooling also modifies the oxide, resulting in a complex mixture of amorphous material and nanocrystalline phases. The MAO process occurs at room temperature in a very dilute and ecologically safe electrolyte. A typical electrolyte might include sodium phosphate, sodium silicate, sodium hydroxide and hydrogen peroxide, at concentrations of less than 5 g/L.[10]

Micro-arc oxidation coating properties depend on the substrate alloy, but also on the electrolyte used and the many parameters of the electrical system.[11] The oxide coatings contain a loose surface layer and underneath, a compact layer. The thickness of the compact layer can reach over 75% of the total coating thickness. After the loose surface layer is ground off, the sample dimension is approximately the same size as the sample before the treatment.[12] Typical alumina coatings consist of a relatively dense polycrystalline layer of alpha-alumina, with a softer, more porous layer of gamma-alumina formed on top. The MAO coatings are very strongly attached to the substrate from which they form. Stress in MAO coatings can be generated via the $\gamma \rightarrow \alpha$ phase transition in alumina.[13,14] The coatings exhibit significant heat-resistance up to 870°C.[14] Typical thermal conductivities are on the order of 1.0 W/m·K, providing good thermal insulation of the substrate material.[15] Polished MAO coatings have a low friction coefficient (0.15 - 0.20).[16] Further, secondary hard particles can be incorporated into the porous coating of MAO.[17]

* *Corresponding author:*
M. Misra
Chemical & Metallurgical Engineering,
University of Nevada-Reno,
1664 N Virginia St., MS 388,
Reno, NV 89557
Phone: 774-784-1603
Emails: misra@unr.edu, kprasadrao@unr.edu

Friction stir processing (FSP) is another recently developed surfacing technique which has attracted attention. It is a modification of friction stir welding (FSW), which is a new technology and is reviewed in detail by Mishra and Ma[18] and Nandan.[19] In FSP, a rotating tool, consisting of a shoulder and a pin, is plunged into the substrate material. The coating obtained by friction stir processing is formed by a hot forging action, as opposed to the melting mechanism inherent in welding and spraying processes. It utilizes the frictional energy dissipated during operation and generates plasticized metal. With the incorporation of secondary particles a surface composite is obtained which is free from melting, solidification, porosity, cracking and micro-segregation. Because of the stirring action in FSP, secondary particles will be uniformly distributed in the substrate material. The surface composite coating is thus a solid phase coating. Further, the surface composite coating obtained by FSP will be an inherent part of the substrate with a sound metallurgical bond. Therefore, the integrity of the coating is ensured and the coating functionally is long lasting, avoiding replacements and repairs which are common with the other methods. Friction stir processing results in microstructural refinement and homogenization due to the large processing strain involved. Apart from surfacing,[20-25] FSP is applied in numerous applications, including grain refinement for superplasticity,[26-30] modification of casting microstructure[31,32] and powder processing.[33-35]

The major issue in attempting to obtain surface composites by FSP is to incorporate secondary particles efficiently and uniformly into the surface of the substrate material. Uniform distribution of secondary particles in aluminum and magnesium alloy substrates has been achieved. Mishra, *et al*.[20] added SiC powder to a small amount of methanol and mixed, and then applied the mixture to the surfaces of the plates to form a thin SiC particle layer. The process was similar to tape casting, except that no binder was added to the mixture. The aluminum plates precoated with the SiC particle layer were subjected to FSP after drying in air.

Most of the other workers[21-24] packed the secondary hard particles into a groove mechanically produced in the substrate surface. Multiwall carbon nanotubes (MWCNTs), SiC particles and Fullerene were incorporated into magnesium and aluminum alloy substrates by forming grooves in the substrates.[21] Single-walled carbon nanotubes were also added to aluminum alloys using friction stir processing.[25] Before friction stir processing, surface "repair" was performed with a modified FSP tool that only had a shoulder and no pin.[24] Zarghani, *et al*.[36] developed Al/Al_2O_3 surface nanocomposite layers by friction stir processing. They found significant improvement in wear resistance in the nanocomposite surfaced aluminum and the wear resistance increased with an increased number of FSP passes attributed to the uniform distribution of nano-sized alumina particles. Mahmud, *et al*.[37] studied the effects of groove design and multipasses on the distribution of SiC particles in the FSP coatings of aluminum alloy. They reported a coating hardness of 110 Hv as compared to 32 Hv for the uncoated substrate material. In view of the increased interest that these two processes have generated among researchers and users, it was deemed worthwhile to compare the performance of these coatings. The objective of this work is to compare the corrosion and wear resistance of MAO-coated aluminum alloys with their FSP counterparts.

Experimental

Ten-mm thick aluminum alloy (Al - 1.86% Mg) was used as the substrate material. The MAO coatings were obtained by applying 400 V direct current between the aluminum anode and titanium cathode in an electrolyte consisting of 25 g/L Na_2SiO_3 and 15 g/L of KOH maintained at 35°C. A 50-min MAO process resulted in a 50-μm thick coating.

For the FSP surface coatings, silicon carbide (SiC) powder (2 - 4 μm size) was used as reinforcement particulates. A groove with a 1-mm depth and 1-mm width was machined on the base plate and SiC powder was manually filled into the groove. Friction stir processing was carried out in the grooves using an H-13 tool steel (60 HRc). The tool shoulder diameter was 16 mm and the pin height and diameter were 1 mm and 2 mm, respectively. Defect-free coatings were obtained by using 2200 RPM and 15 mm/min speed.

Scanning electron microscopy (SEM) with an EDS attachment was used to study the chemical composition of the coatings and the wear and corrosion characteristics of the samples. X-ray diffraction (XRD) analysis was performed to assess the phases formed in the coatings.

The MAO coating hardness was evaluated using the Knoop hardness test (200-g load) as the coatings were very thin. The FSP coating hardness used the Vickers hardness test (500-g load).

The corrosion resistance was assessed by electrochemical impedance spectroscopy (EIS) (ASTM-B457) in a 3.5% NaCl solution. The higher the impedance value at the lowest frequency, the better the corrosion resistance. Salt spray testing (ASTM-B117) was conducted for 1000 hr on uncoated and MAO-coated samples. In the salt-spray testing, the macro surface appearance and weight loss were used as criteria in evaluating corrosion resistance.

The wear resistance of the coatings was assessed with a custom-built pin-on-disk test (ASTM-G99). Coated and uncoated aluminum alloy specimens were used as pins (10-mm height, 6-mm diameter) which were tested against SiC paper attached to a steel disk. The disk (15-mm diameter) was rotated at 200 RPM. A 10 N load was applied to the pin and the test duration was 15 min.

Results and discussion

Coating morphology, chemistry and microstructure

1. MAO Coatings

The typical surface morphology of an MAO-coated sample is shown in Fig. 1. A porous coating was found to be formed on the surface of the aluminum alloy. Many small pores were observed, presumably corresponding to fine arcing on the sample surface during the process. It has been proposed[38] that there is an instantaneous temperature rise in the micro-arc zone (~104 K), which causes aluminum to melt, leading to the eruption of partial molten alumina along many small discharge channels, forming a loose layer with high porosity on the surface. The coating thickness gradually increases with oxidation time, but the breakdown of the

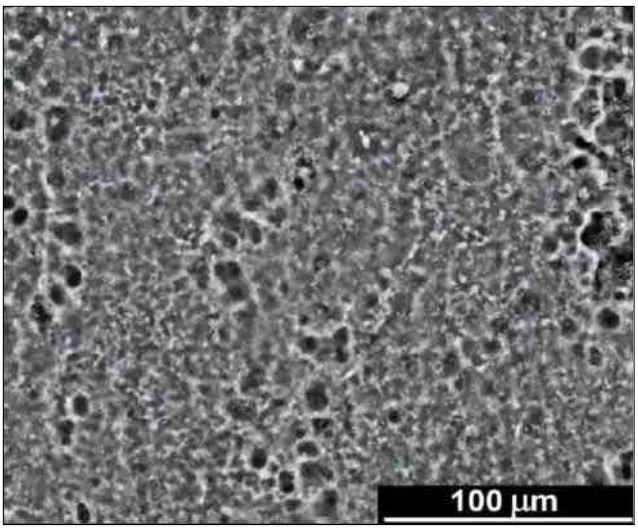

Figure 1—*Surface morphology of an MAO coating.*

coating becomes more and more difficult. Spark discharges in the coating still continue, and promote continuing growth of the oxide ceramic coating into the aluminum substrate, after which a compact layer is formed.[39] In our work, we achieved a coating thickness of ~50 μm after 50 min of oxidation.

The chemical composition of the MAO coatings, as evaluated by SEM-EDS, showed significant inward diffusion of O_2 (21.95%) in the coatings. When plasma discharge occurs in the ceramic coatings, oxygen can be delivered directly into the internal layers of the ceramic coatings through the discharge channels. Oxygen-permeating oxidation into the aluminum substrate plays a leading role in coating growth, and the growth rate of the MAO coating is controlled by the rate of oxygen transfer into the aluminum substrate. The instantaneous high temperature and high pressure in the microarc zone greatly enhance interdiffusion between the oxygen anions and aluminum cations in the coating near the discharge zones. Oxygen anion transfer is enhanced towards the aluminum substrate due to the higher electric field intensity of 106 V/cm in the coating.[39]

The chemical composition study also showed silicon present in the MAO coating. As the substrate material did not contain silicon, it could only originate from the electrolyte. The tendency of the silicon concentration to increase at the coating/electrolyte interface has been reported by Monfort, *et al*.[40] Several previous studies have considered the incorporation of electrolyte species into the anodic material via conventional anodic oxidation.[41-43] In conventional anodic oxidation, the incorporated electrolyte species would be immobile, migrate inward or migrate outward within the coating under the electric field. The incorporation of electrolyte species into the coating can be regarded as a series of processes as follows:

1. Transport of anions from the bulk electrolyte into the diffusion layer;
2. Transport of the anions across the diffusion layer to the coating/electrolyte interface;
3. Adsorption of the anions on the film surface and
4. Incorporation of the adsorbed anion into the coating.[41]

In the silicate electrolyte system, $SiO_3^=$ ions are transported to the coating/electrolyte interface.** Therefore gel layers may form at the coating/electrolyte interface to prevent the incorporation of electrolyte species. Furthermore, SiO_2 may fuse with Al_2O_3 at high temperatures (2×10^3 to 3×10^3°C),[9] forming a mullite phase on the coating surface. Therefore, silicon elements are mostly precipitated in the outer region of the coating and are regarded as immobile species.

The x-ray diffraction pattern of the MAO coating (Fig. 2) shows the formation of Al_2O_3 along with SiO_2, Al_2SiO_5 (kainite) and $Al_6Si_2O_{13}$ (mullite). Magnesium-containing additive was found to intensify mullite formation in a kaolin briquette.[44] In MAO processes, the alumina is produced at both the metal/coating and coating/electrolyte interfaces as a result of migration of $O^=$, OH^- and Al^{+3} ions across the coating assisted by a high electric field (106 to 108 V/m).[9] Rama Krishna, *et al*.[45] reported that with increasing silicon content, the corresponding mullite phase also increases. The presence of SiO_2, Al_2SiO_5 and $Al_6Si_2O_{13}$ indicate that silicate ions in the electrolyte take part in the formation of the coating. In aqueous solution, the sodium silicate is easily hydrolyzed to form $Si(OH)_4$, which will subsequently be dehydrated to SiO_2 through a series of reactions.[46] SiO_2 can also form thru direct oxidation of SiO_4^{-4} under high electric field and high temperature conditions.[47] The high temperature generated by the plasma discharge can cause amorphous silicon oxides to diffuse into the metastable γ-Al_2O_3 phase in the molten condition, resulting in the formation of the mullite phase.[48]

2. FSP Coatings

Figure 3 shows the particle distribution in the finer FSP nugget. No significant change in size and shape of the SiC particles was noted after FSP. In the FSP nugget, a significantly large number of the particles retained their original size and shape. This could be related to a lower shearing load on the particles. Also, the particles were found to be uniformly distributed.

The combined effect of the downward flow near the probe by the thread action and the upward flow on the advancing side probably enhanced the flow that carried the powder on the retreating side of the probe toward the advancing side, and contributed to the wider distribution of the powder in the nugget zone.[37] The thickness of the FSP surface coating was found to be about 1.0 mm. Analysis of the chemical composition of the FSP coating indicated the presence of a small amount of oxygen (1.5%) and iron (0.6%) in addition to Si, C, Mg and Al. Oxygen pick-up was attributed to the higher temperatures generated during FSP. The pick up of small amounts of iron could be related to tool wear.

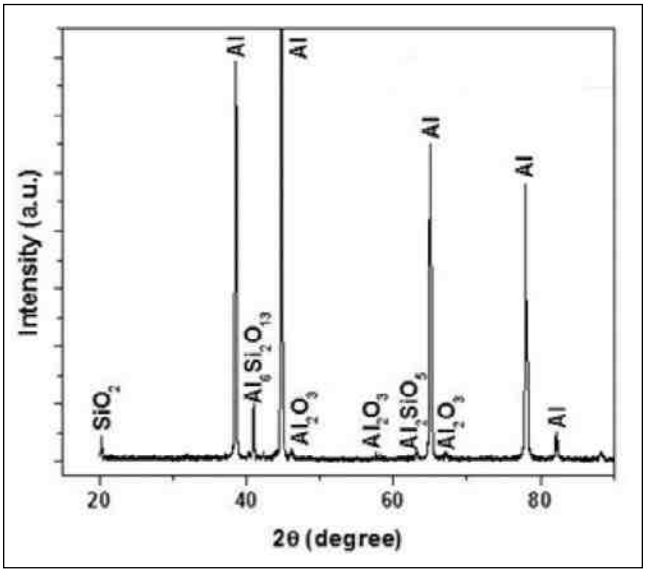

Figure 2—*X-ray diffraction pattern for an MAO coating.*

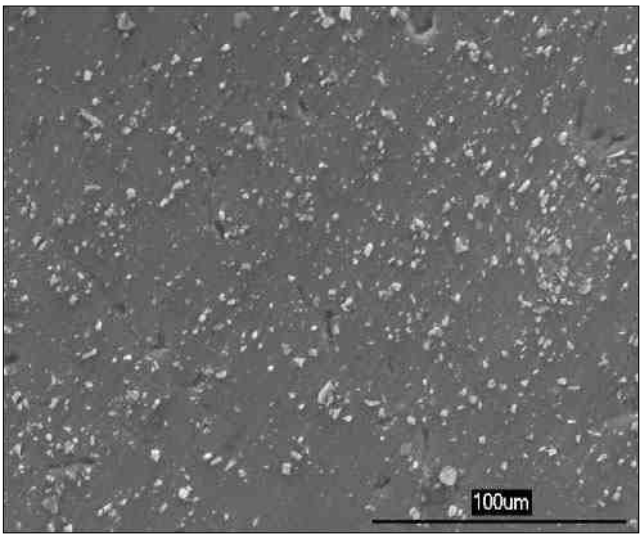

Figure 3—*Surface morphology of an FSP coating.*

***There may be some unstable $HSiO_3$- ions in the electrolyte but they will decompose at the film surface due to the high electric field.*

As seen in Fig. 4, the XRD results showed the presence of SiC and aluminum. Since FSP is a solid state process, some mechanical alloying may take place and there is a possibility of some new phase formation. However, in our work, we did not notice any new phase formation other than that of the matrix material and particulates.

Hardness and wear

The hardness of the uncoated aluminum alloy was 60 HV_{500}. The MAO coating exhibited a hardness value of 2100 HK_{200}, whereas the FSP coating hardness was 258 HV_{500}. The relatively high hardness of the MAO coating was attributed to the formation of harder phases such as Al_2O_3, SiO_2, Al_2SiO_5 (kainite) and $Al_6Si_2O_{13}$ (mullite). The increase in hardness for the FSP coatings was attributed to the homogenous distribution of the SiC particles in the processed zone. Rotation speed was found to be a major factor controlling the particulate dispersion in the nugget zone rather than the heat input and temperature of the nugget zone.[37] The results are significant in the sense that one can get harder coatings by the MAO technique versus the FSP technique.

Pin-on-disk tests showed that the wear loss of uncoated aluminum alloy was 250 mg whereas that of MAO coatings was nil. The FSP coated samples showed 8 mg weight loss. The uncoated sample showed deep, wide wear tracks (Fig. 5a) whereas the FSP coated sample (Fig. 5b) showed relatively thin and shallow wear tracks. In the case of the MAO coatings, no such wear tracks were observed (Fig. 5c). The excellent wear resistance of the micro-arc oxidation coating was attributed to the formation of relatively harder oxide phases and silicates. The increased wear resistance of the FSP coatings could be attributed to the dispersed hard particles with in the soft matrix.

If these composite coatings were to be developed by melting techniques, they would not be acceptable for many applications. For example, aluminum silicon carbide composites are not suitable for a wide range of applications because of their low fracture toughness and poor fatigue properties.[49-51] Brittle interfacial reactions which are lower in strength than the reinforcing particles may be responsible for the lower fracture toughness of melt-formed MMC.[52] Both cast and powder metallurgy-formed metal matrix composites (MMC) suffer from agglomeration problems. Their toughness and fatigue properties can be improved by reducing particle agglomeration and interfacial reactions between the matrix and the reinforcing particles. Coatings obtained by solid state processing such as FSP are free from such melting and interfacial reactions and therefore are free from metallurgical and physical problems associated with melting techniques.

Corrosion resistance

Figure 6 shows typical Bode plots for uncoated and coated samples. The impedance values from this plot at the lower frequency value are tabulated in Table 1.

Impedance values of uncoated and FSP-coated samples were in the range of 100 to 180 Ω, whereas MAO-coated samples showed impedance values several orders of magnitude greater than either the uncoated or FSP-coated samples. In view of the high imped-

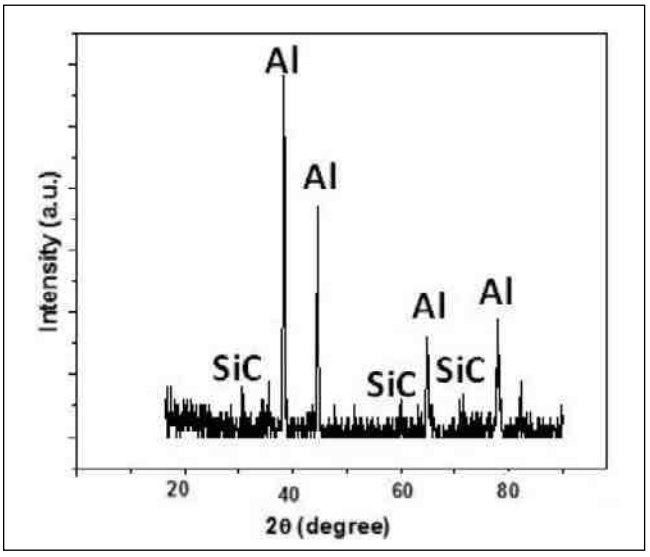

Figure 4—*X-ray diffraction pattern for an FSP coating.*

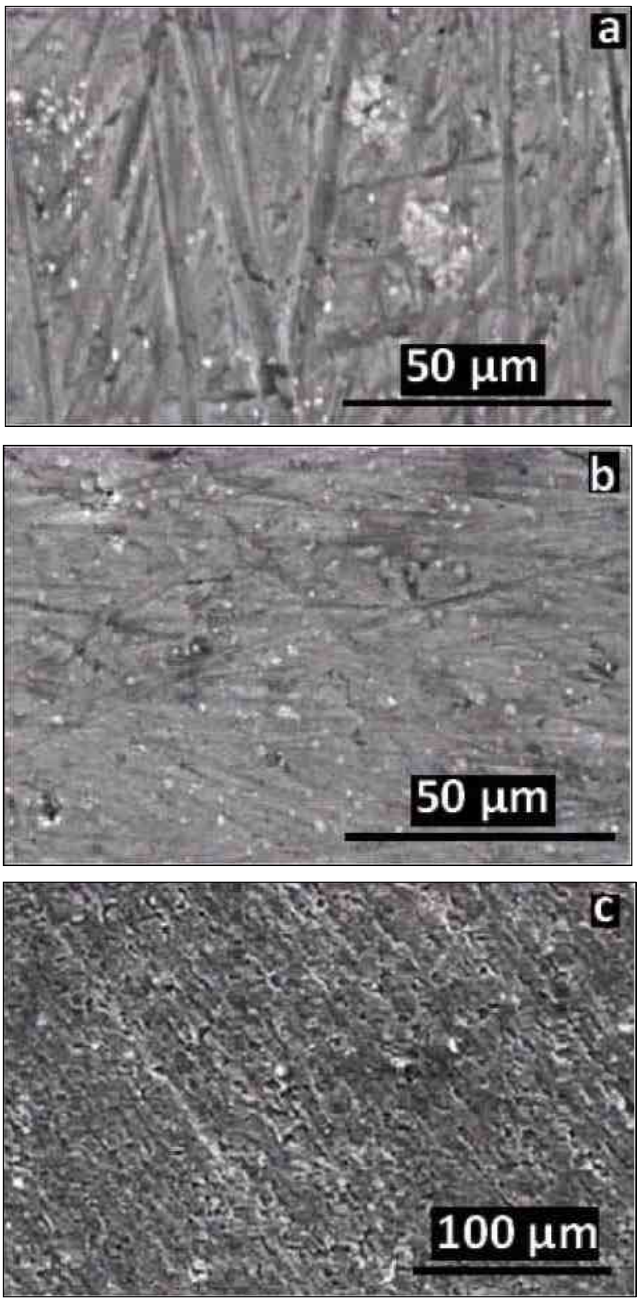

Figure 5—*Wear tracks on (a) uncoated, (b) FSP-coated and (c) MAO-coated samples.*

Table 1

Impedance values at the lowest frequency

Impedance (Ω)		
Uncoated	MAO-coated	FSP-coated
100	12×10^7	180

ance values exhibited by the MAO coating, salt spray testing was performed and the results were compared with uncoated samples. In the salt spray test, the MAO-coated samples showed no weight loss, whereas the uncoated samples showed a corrosion rate of 336.5 mpy. Visual examination of the surface attack corroborated the weight loss data (Fig. 7). Uncoated samples corroded significantly whereas the MAO-coated sample surface was found to be intact, indicating superior corrosion resistance.

The higher corrosion resistance of the MAO coatings can be attributed to the formation of phases such as Al_2O_3, SiO_2, Al_2SiO_5 (kainite) and $Al_6Si_2O_{13}$ (mullite), which are known to exhibit better corrosion resistance. The magnesium in Al-Mg alloys has been found to enhance mullite formation. As the electrolyte used is predominantly silicate, amorphous material would have formed in the coating, particularly at the interface.[53]

In summary, it can be inferred that for relatively moderate wear resistance, FSP coatings can be used. For applications involving relatively high wear resistance, MAO coatings are recommended. MAO coatings are also useful for applications involving high corrosion resistance. They are also useful for applications where both high wear and high corrosion resistance are required. Therefore, it might be feasible to use MAO-coated aluminum alloys as the structural materials requiring excellent corrosion- and wear-resistance.

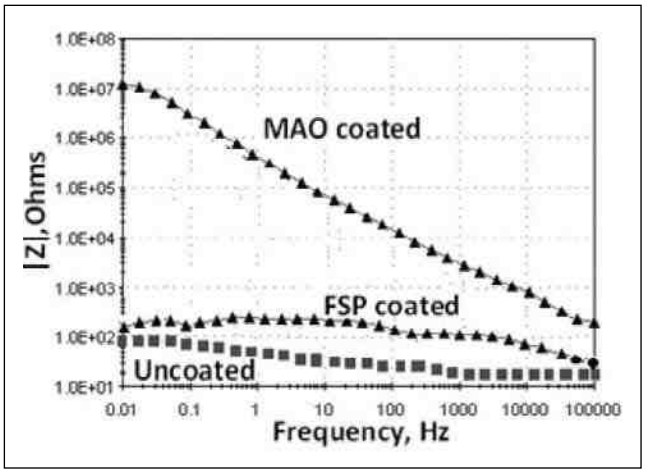

Figure 6—*Bode plots of uncoated, FSP-coated and MAO-coated samples.*

Conclusions

1. Coatings on aluminum alloys obtained either by friction stir processing or micro-arc oxidation improved wear resistance.

2. The wear and corrosion resistance imparted by micro-arc oxidation coatings are far superior to those obtained with friction stir processing.

Acknowledgement

This work was supported by funding received from the U.S Department of Energy through the contract # DE-FC07-06-ID14782.

References

1. O. Khaselev, D. Weiss & J. Yahalom, *Corros. Sci.*, **43** (7), 1295 (2001).
2. Y. Zhang, *et al.*, *Surf. Coat. Technol.*, **161** (1), 36 (2002).
3. Y. Ma, *et al.*, *Thin Solid Films*, **469-470**, 472 (2004).
4. H. Hsiao & W. Tsai, *Surf. Coat. Technol.*, **190** (2-3), 299 (2005).
5. X.Nie, *et al.*, *Surf. Coat. Technol.*, **116-119**, 1055 (1999).
6. A.L. Yerokhin, *et al.*, *J. Physics D: Appl. Phys.*, **36** (17), 2110 (2003).
7. A.A. Voevodi, *et al.*, *Surf. Coat. Technol.*, **86-87** (2), 516 (1996).
8. A.L.Yerokhin, *et al.*, *Surf. Coat. Technol.*, **130** (2-3), 195 (2000).
9. A.L.Yeroklin, *et al.*, *Surf. Coat. Technol.*, **122** (2-3), 73 (1999).
10. J. Curran, *Plasma Electric Oxide Coatings*, University of Cambridge, Cambridge, UK; www.msm.cam.ac.uk/mmc/people/old/jac/james.html (last accessed 11/07/09).
11. A. Bai & Z-J. Chen, *Surf. Coat. Technol.*, **203** (14), 1956 (2009).
12. W. Xue, *et al.*, *Thin Solid Films*, **372** (1-2), 114 (2000).
13. R.H.U. Khan, *et al.*, *Surf. Coat. Technol.*, **200** (5-6), 1580 (2005).
14. S.V. Gnedenkov, *et al.*, *Surf. Coat. Technol.,* **123** (1), 24 (2000).
15. M.V. Gerasimov , *Metallurgist*, **51** (11-12), 677 (2007).
16. J. Baxi, *et al.*, *Vacuum*, **83** (1), 217 (2008).
17. R. Arrabal, *et al.*, *J. Mater. Sci.*, **43** (5), 1532 (2008).
18. R.S. Mishra & Z.Y. Ma, *Mater. Sci. Eng. R*, **50** (1-2), 1 (2005).

Figure 7—*Salt spray tested MAO-coated and uncoated specimens.*

19. R. Nandan, T. DebRoy & H.K.D.H. Bhadeshia, *Prog. Mater. Sci.*, **53** (6), 980 (2008).
20. R.S. Mishra, Z. Y. Ma & I. Charit, *Mater. Sci. Eng. A*, **341** (1-2), 307 (2003).
21. Y. Morisada, *et al.*, *Mater. Sci. Eng. A*, **419** (1-2), 344 (2006).
22. Y. Morisada, *et al.*, *Mater. Sci. Eng. A*, **433** (1-2), 50 (2006).
23. Y. Morisada, *et al.*, *Composites Part A,* **38** (10), 2097 (2007).
24. C.J. Lee, J.C. Huang & P.J. Hsieh, *Scripta Mater.*, **54** (7), 1415 (2006).
25. L. B. Johannes, *et al.*, *Nanotechnology*, **17** (12), 3081 (2006).
26. R. S. Mishra, *et al.*, *Scripta Mater.*, **42** (2), 163 (2000).
27. Z. Y. Ma, R. S. Mishra & M.W. Mahoney, *Acta Mater.*, **50** (17), 4419 (2002).
28. I. Charit & R. S. Mishra, *Acta Mater.*, **53** (15), 4211 (2005).
29. Z. Y. Ma, *et al.*, *Mater. Sci. Eng. A*, **351** (1-2), 148 (2003).
30. P. Cavaliere & P.P. de Marco, *J. Mater. Process. Technol.*, **184** (1-3), 77 (2007).
31. Z.Y. Ma, S.R. Sharma & R.S. Mishra, *Mater. Sci. Eng. A*, **433** (1-2), 269 (2006).
32. K. Nakata, *et al.*, *Mater. Sci. Eng. A*, **437** (2), 274 (2006).
33. C.J. Hsu, P.W. Kao & N.J. Ho, *Scripta Mater.*, **53** (3), 341 (2005).
34. C.J. Hsu, *et al.*, *Acta Mater.*, **54** (19), 5241 (2006).
35. C.J. Hsu, P.W. Kao & N.J. Ho, *Mater. Lett.*, **61** (6), 1315 (2007).
36. A. Shafiei-Zarghani, S.F. Kashani-Bozorg & A. Zarei-Hanzaki, *Mater. Sci. Eng. A*, **500** (1-2), 84 (2009).
37. E.R.I. Mahmoud, K. Ikeuchi & M. Takahashi, *Sci. Technol. Weld. Joining*, **13** (7), 607 (2008).
38. L.A. Yerokhin,V.V. Lyubimov & V.R. Ashitkov, *Ceram. Int.*, **24** (1), 1 (1998).
39. W. Xue, *et al.*, *Thin Solid Films*, **372** (1-2), 114 (2000).
40. F. Monfort, *et al.*, *J. Electrochem. Soc.*, **152** (6), C382 (2005).
41. P. Skeldon, *et al.*, *Philos. Mag. B*, **72** (4), 391 (1995).
42. G.C. Wood, *et al.*, *J. Electrochem. Soc.*, **143** (1), 74 (1996).
43. G. Lv, *et al.*, *Appl. Surf. Sci.*, **253** (5), 2947 (2006).
44. Z.A. Livson & E.D. Lisovaya, *Refract. Ind. Ceram.*, **11** (5-6), 384 (1970).
45. L. Rama Krishna, *et al.*, *Metall. Mater. Trans. A*, **38** (2), 370 (2007).
46. V. Birss, *et al.*, *J. Electrochem. Soc.*, **151** (1), B1 (2004).
47. O. Khaselev, D. Weiss & J. Yahalom, *J. Electrochem. Soc.*, **146** (5), 1757 (1999).
48. S-G. Xin, *et al.*, *Mater. Chem. Phys.*, **97** (1), 132 (2006).
49. A.K. Vasudévan & K. Sadananda, *Metall. Mater. Trans. A*, **26** (12), 3199 (1995).
50. B. Roebuck, *J. Mater. Sci. Lett.*, **6** (10), 1138 (1987).
51. M.P. Thomas & J.E. King, *Mater. Sci. Technol.*, **9**, 742 (1993).
52. K.S. Foo, *et al.*, Composites, **25** (7), 677 (1994).
53. J.A. Curran & T.W. Clyne, *Surf. Coat. Technol.*, **199** (2-3), 168 (2005).

About the authors

Sudhir Baral *is a graduate research assistant at the Department of Chemical and Materials Engineering, University of Nevada, Reno, Nevada. He obtained a B.S degree in Metallurgical Engineering from the University of Idaho, Moscow, Idaho in 2008.*

Raghu Raj Rangaraju *is a graduate research assistant at the Department of Chemical and Materials Engineering, University of Nevada, Reno, Nevada. He obtained a B.E degree in Chemical Engineering from Bangalore University, India and worked in the biotechnology industry as a process engineer before moving to the USA.*

Anand Patil *is a graduate teaching assistant at the Department of Chemical and Materials Engineering, University of Nevada, Reno, Nevada. He obtained a B.E degree in Metallurgical Engineering from the University of Pune, India in 2008.*

Dr. Prasad Rao Kalvala *is a Professor and is in-charge of the Materials Joining Laboratory, Department of Metallurgical and Materials Engineering , Indian Institute of Technology - Madras (IIT Madras) , Chennai , India. He received his Ph.D. from IIT Madras in the area of welding metallurgy in 1983 .*

Dr. K. S. Raja *is a Research Professor at the Department of Chemical and Materials Engineering, University of Nevada, Reno, Nevada. He received his B.E degree in Mechanical Engineering from Anna University, Chennai in 1986 and M.Tech (1988) & Ph.D (1993) degrees in Metallurgical Engineering from IIT, Madras, India.*

Dr. Manoranjan Misra *is a Professor of Materials Engineering, University of Nevada, Reno, Nevada. He received his Ph.D degree in Metallurgical Engineering from the University of Utah, Salt Lake City, Utah in 1981. Currently, he is the Director of the Renewable Energy Center of the University of Nevada, Reno.*